

Spectra and M1 Decay Widths of Heavy-Light Mesons

T.A. Lähde*, C.J. Nyfält† and D.O. Riska‡

February 22, 2000

Department of Physics, POB 9, 00014 University of Helsinki, Finland

Abstract

The M1 decay widths of charm and bottom mesons and their excited states are sensitive to the relativistic aspect of the quark current operators and obtain a significant contribution from the interaction current that is associated with the scalar confining interaction between heavy quarks (Q) and light antiquarks (\bar{q}). Consequently they provide direct evidence on the latter. The spectra and the M1 transition widths of the D , D_s and B , B_s mesons and their orbital excitations are calculated here within the framework of the Blankenbecler-Sugar equation, which allows a covariant treatment, while retaining a formal similarity to the nonrelativistic approach. The hyperfine interaction in the $Q\bar{q}$ mesons is modeled by screened gluon exchange, which shares many features with the instanton induced interaction. The quality of the model is tested by calculation of the spectra and M1 decay widths of charmonium.

*talahde@rock.helsinki.fi

†nyfalt@rock.helsinki.fi

‡riska@science.helsinki.fi

1 Introduction

A dynamical description of the spectrum of the heavy flavor mesons $Q\bar{q}$ has *a priori* to be relativistic as the confined light quarks and antiquarks have velocities close to that of light. Combination of this requirement, with the non-relativistic instantaneous aspect of the effective linear [1] (or near linear [2]) confining interaction suggests that a 3-dimensional quasipotential reduction of the Bethe-Salpeter equation should provide the most obvious framework for a realistic description. This is *a fortiori* the case as the Bethe-Salpeter equation with instantaneous interactions, while commonly employed, [3], fails to provide satisfactory results for the M1 transitions of the analogous heavy quarkonia [4].

Among the many choices of quasipotential equations the Blankenbecler-Sugar equation [5, 6] suggests itself because of its transparent formal similarity to the nonrelativistic Lippmann-Schwinger equation, to which it reduces in the adiabatic limit. Moreover it admits direct employment of the conventional (relativistic) models for the hyperfine interaction between quarks and antiquarks, as well as the linear confining interaction along with its obvious relativistic modifications. The key advantage of the Blankenbecler-Sugar equation over the nonrelativistic or “relativized” versions of the nonrelativistic wave equation is the unapproximated treatment of the relativistic two-particle kinetic energy operator of the $Q\bar{q}$ system. The relativistic modifications to the interaction are in comparison modest, and may be treated in an approximate fashion, when convenient. This feature is shared with the Gross [7] reduction of the Bethe-Salpeter equation, which has been applied to heavy flavor mesons in ref.[8].

Given this situation, several different versions of the Blankenbecler-Sugar equation have been employed in the literature [9]. We shall here use the symmetrical version of ref. [10] to calculate both the spectra and the M1 decay widths of the D and D_s as well as the B and B_s mesons and their orbital excitations. The formalism then differs somewhat from that used to describe the $Q\bar{q}$ system in refs. [11]. The main advantage of the version used here is that it leads to a Lippmann-Schwinger type wave-equation. It differs most obviously from that used in refs.[11] in the appearance of the “minimal relativity” [12] square root factors $\sqrt{m/E}$ in the effective interaction potential in the wave equation.

The radiative transitions of the ground state $Q\bar{q}$ mesons may be described phenomenologically by effective field theory methods [13, 14, 15]. A complete dynamical model is however required for any comprehensive description of the decays of the full spectrum of $Q\bar{q}$ states. The static quark model is insufficient here, as it is expected to overpredict the width of the M1 transition for $D^{+*} \rightarrow D^+\gamma$ by a large factor in analogy to its large overprediction of the width for the M1 decay $J/\psi \rightarrow \eta_c\gamma$, and which is resolved only by employment of the relativistic magnetic moment operator for the heavy quarks along with the interaction current operator that is associated with the scalar confining interaction [16].

In comparison to heavy quarkonia the heavy-light $Q\bar{q}$ mesons are more complex systems in view of the still unsettled form of the hyperfine interaction for the light quarks and concomitantly their empirically still only poorly known spectrum. While the branching ratios of the M1 decays of the charmed vector mesons are known, their still unknown total decay widths prevent an absolute empirical determination of their M1 decay widths. In spite of – and because of – this situation it remains a challenge to decode the structure and the dynamics of these systems, as this is a main key to the understanding of the nature of the

confining interaction and the hyperfine interaction between constituent quarks.

There are good theoretical [1, 17] and phenomenological [16] reasons to expect the confining interaction to be linear with a scalar spinor structure, although mixtures of combinations of scalar and vector coupling terms continue to be employed [3, 11]. For the heavy light $Q\bar{q}$ systems the hyperfine interaction is likely to be formed as a combination of the screened perturbative gluon exchange interaction [18] and the direct instanton induced interaction [19], which share many qualitative features. The latter appears in the instanton liquid model description of the QCD vacuum [20], which is supported by numerical lattice calculations [21, 22]. In the case of heavy light quarkonia the relativistic corrections to the gluon exchange interaction cause an appreciable damping of that interaction, besides the screening of the the color hyperfine coupling strength.

We here consider the M1 decay rates of the $Q\bar{q}$ systems, because these are expected to be overpredicted by the static quark model, and are likely to provide decisive information on the nature of the confining interaction. Because the constituent quark masses appear in different combinations in the magnetic transition operators for the different charge states of the $Q\bar{q}$ mesons the M1 transition rates should also provide information on the constituent quark masses. We show that the decay rates predicted by the static quark model for the M1 transition $D^* \rightarrow D\gamma$ is strongly reduced with (1) employment of the relativistic magnetic moment operator for the quarks in combination with (2) the interaction current, that appears if the confining interaction couples as a scalar. This result falls in line with that for the corresponding M1 decay rate problem of heavy quarkonia [16]. For $q\bar{q}$ systems (i.e. systems with equal quark and anti-quark masses) neither the gluon exchange interaction nor the instanton induced interaction gives rise to any two-body current operator with a spin-flip part. The spin-flip component of those exchange current operators that appear in the case of $Q\bar{q}$ systems usually have much smaller matrix elements compared to the matrix elements of the two-body current that is associated with the scalar confining interaction.

The effective interaction potential between the heavy quark and the light antiquark is accordingly described by a scalar linear confining + one-gluon exchange interaction with a hyperfine interaction formed of the perturbative gluon exchange interaction. The parameters of this model are, to the extent possible, fixed to values obtained by lattice calculations as well as to the known part of the D and D_s meson spectra, and then appropriately scaled to the bottom mesons. Finally the quality of the model is tested by a calculation of the spectrum and the M1 decay widths of charmonium.

With the framework of the Blankenbecler-Sugar equation and the $Q\bar{q}$ interaction models above it is possible to obtain spectra for both charmonium and the heavy-light mesons, which agree overall with the empirical spectra, where these are known. Similarly the description of the (known) M1 decay rates of the J/ψ and the ψ' are well described. The M1 decay rates for the D and B mesons are predictions, as absolute empirical determination of these are yet to be made. The present result that it is possible to achieve a satisfactory description of both the spectra and M1 decay rates of heavy quarkonia and heavy light mesons differs from that of ref.[23]. The key point here is the employment of an unapproximated quark current operator.

This report falls into 7 sections. Section 2 contains a description of the application of the Blankenbecler-Sugar equation to the $Q\bar{q}$ and $Q\bar{Q}$ systems. Section 3 contains a description of the interaction parts of the Hamiltonian and

the current operators. The calculated D, D_s and B, B_s meson as well as the $c\bar{c}$ spectra are described in section 4. Section 5 describes the quark current operators, including the two-quark current that arises along with a linear scalar confining interaction. The calculated M1 transition rates are reported in section 6. Section 7 contains a concluding discussion.

2 The Blankenbecler–Sugar equation applied to $Q\bar{q}$ systems

The Blankenbecler–Sugar equation for a $Q\bar{q}$ system may be expressed as an eigenvalue equation of the form

$$\left(\frac{\vec{p}^2}{2m_r} + V\right)\psi = \epsilon\psi. \quad (1)$$

Here m_r is the reduced mass of the heavy quark (Q) mass M and the light antiquark (q) mass m : ($m_r = Mm/(M+m)$). The the eigenvalue ϵ is related to the energy E of the $Q\bar{q}$ meson system as

$$\epsilon = \frac{[E^2 - (M-m)^2][E^2 - (M+m)^2]}{8m_r E^2}. \quad (2)$$

The interaction operator V , which need not be a local operator, may be obtained from the $Q\bar{q}$ irreducible quasipotential \mathcal{V} (in momentum space) as [24]:

$$V(\vec{p}', \vec{p}) = \sqrt{\frac{M+m}{W(\vec{p}')}} \mathcal{V}(\vec{p}', \vec{p}) \sqrt{\frac{M+m}{W(\vec{p})}}. \quad (3)$$

Here the function W is defined as

$$W(\vec{p}) = E_Q(\vec{p}) + E_{\bar{q}}(\vec{p}), \quad (4)$$

with $E_Q(\vec{p}) = \sqrt{M^2 + \vec{p}^2}$ and $E_{\bar{q}}(\vec{p}) = \sqrt{m^2 + \vec{p}^2}$ respectively. In the Born approximation the quasipotential \mathcal{V} equals the $Q\bar{q}$ invariant scattering amplitude \mathcal{T} , and thus a constructive relation to field theory obtains.

Numerical solution of the wave equation (1) yields a value for the eigenvalue ϵ . The energy (rest mass) of the $Q\bar{q}$ meson is then obtained as

$$E = \sqrt{M^2 + m^2 + 4m_r\epsilon + 2\sqrt{M^2m^2 + 2m_r(M^2 + m^2)\epsilon + 4m_r^2\epsilon^2}}. \quad (5)$$

In the equal mass case $M = m$ this expression reduces to $E = \sqrt{4m(m + \epsilon)}$.

The relation between the (total) energy E of the $Q\bar{q}$ system and the eigenvalue ϵ in the equation (1) shows that the relativistic treatment of the kinetic energy term in the Hamiltonian leads to a lowering of the former in comparison to what a nonrelativistic treatment would have implied. This is a consequence of the effective weakening of the repulsive kinetic energy operator, that results when the quadratic p^2 terms are replaced by square roots of p^2 . Despite the formal similarity between the Blankenbecler–Sugar equation and the Schrödinger equation, the former employs a quadratic mass operator.

The main component of the interaction between the Q and \bar{q} quarks is the linear confining interaction, which is well defined only in the position space representation, which we shall therefore adhere to. While the Blankenbecler–Sugar equation takes full account of the relativistic two-quark kinetic energy operator, the relativistic aspects of the hyperfine interaction operators will be treated perturbatively. This treatment is more than adequate for the heavy quark, but less so for the light one. It does, however, allow retention of the conventional operator structure of the interaction operator between the quarks.

3 The Interaction Hamiltonian for $Q\bar{q}$ systems

3.1 The confining interaction

The linear confining interaction will here – on the basis of compelling indications – be assumed to be a scalar in the spinor representation [16, 17]. To second order in the inverse quark masses this interaction, as calculated from the invariant amplitude according to (3), takes the form

$$V_C = cr \left(1 - \frac{3\vec{p}^2}{2m_2^2} \right) + \frac{c}{4Mmr} - \frac{c}{r} \frac{M^2 + m^2}{4M^2m^2} \vec{S} \cdot \vec{L} + \frac{c}{r} \frac{M^2 - m^2}{8M^2m^2} (\vec{\sigma}_Q - \vec{\sigma}_{\bar{q}}) \cdot \vec{L}. \quad (6)$$

Here c is the string tension parameter, the value of which is ~ 1 GeV/fm. The mass coefficient m_2 is defined as

$$\frac{1}{m_2} = \frac{\sqrt{M^2 + m^2 + Mm}}{\sqrt{3}Mm}. \quad (7)$$

The spin-independent term that is proportional to $1/r$ is a consequence of the square root factors in (3). Without those factors the factor $3/2$ in the momentum dependent term in the first bracket on the r.h.s. of (6) would be 1. The terms of second order in the inverse quark masses in (6) are implied by scalar coupling for the confining interaction. As the antisymmetric spin-orbit interaction has no diagonal matrix elements between any of the states in the S - and P -shells, and only connects spin singlet and triplet states with $J = L$ it contributes to the energy only at quartic order in the inverse quark masses.

The term of second order in \vec{p} in the spin-independent term in (6) is unrealistically large for light quarks, but is substantially moderated by inclusion of the next term in the (asymptotic) $(v/c)^2$ expansion. Similarly the spin-orbit interaction in (6) is unrealistically large for light quarks. Both of these explicitly velocity dependent terms are strongly moderated by the higher order terms in the (asymptotic) expansion in \vec{v}^2 . This is seen directly by comparison to the corresponding terms in the quartic correction term to (6), which takes the form

$$V_C^{(4)} = -\frac{c\pi}{16m_{4a}^4} \delta^{(3)}(r) - \frac{c}{r} \frac{\vec{p}^2}{16m_{4b}^4} - \frac{c}{r} \frac{(\vec{p}^2 - (\hat{r} \cdot \vec{p})^2)}{32m_{4c}^4}$$

$$\begin{aligned}
& + cr \frac{3}{8} \frac{\vec{p}^4}{m_{4d}^4} + \left\{ \frac{c}{32r^3} \left[\frac{1}{M^3} \left(\frac{3}{M} + \frac{2}{m} \right) + \frac{1}{m^3} \left(\frac{3}{m} + \frac{2}{M} \right) \right] \right. \\
& + \frac{c}{8r} \frac{\vec{p}^2}{M^2 m^2} \left(5 + \frac{3}{2} \left(\frac{M}{m} \right)^2 + \frac{3}{2} \left(\frac{m}{M} \right)^2 \right) \left. \right\} \vec{S} \cdot \vec{L} \\
& + \frac{1}{16M^2 m^2} \frac{c}{r^3} Q_{12}.
\end{aligned} \tag{8}$$

where Q_{12} is the quadratic spin-orbit interaction operator

$$Q_{12} = (\vec{\sigma}_Q \cdot \vec{L} \vec{\sigma}_{\bar{q}} \cdot \vec{L} + \vec{\sigma}_{\bar{q}} \cdot \vec{L} \vec{\sigma}_Q \cdot \vec{L})/2. \tag{9}$$

The quartic component of the antisymmetric spin-orbit interaction has been dropped here, as it contributes to the energies of the meson states only to sixth order. Above the mass coefficients m_{4j} are defined as

$$\frac{1}{m_{4a}^4} = \left[\frac{(M+m)^2}{M^3 m^3} - \frac{1}{M^2 m^2} \right] \tag{10}$$

$$\frac{1}{m_{4b}^4} = \left[\frac{3(M+m)^4}{M^4 m^4} - \frac{8(M+m)^2}{M^3 m^3} \right] \tag{11}$$

$$\frac{1}{m_{4c}^4} = \left[\frac{5(M+m)^4}{M^4 m^4} - \frac{16(M+m)^2}{M^3 m^3} + \frac{2}{M^2 m^2} \right] \tag{12}$$

$$\frac{1}{m_{4d}^4} = \left[\frac{(M+m)^4}{M^4 m^4} - \frac{3(M+m)^2}{M^3 m^3} + \frac{1}{M^2 m^2} \right] \tag{13}$$

The scalar structure of the confining interaction implies functional relations between the different spin components of the potential. Thus e.g. in the static limit the spin-orbit component may be calculated from the central component as

$$v_{LS}(r) = -\frac{1}{4} \left(\frac{1}{M^2} + \frac{1}{m^2} \right) \frac{1}{r} \frac{\partial}{\partial r} v_c(r). \tag{14}$$

Here $v_c(r)$ is the central confining potential and $v_{LS}(r)$ is the coefficient function for the spin-orbit coupling operator $\vec{S} \cdot \vec{L}$. When the static limit is not invoked, the corresponding relation is more complicated. To a good approximation it may however be cast in the form

$$\begin{aligned}
v_{LS}(r) &= -\frac{2c}{\pi r} \frac{\partial}{\partial r} \int_0^\infty dr' r'^3 \\
& \int_0^\infty dk k^2 j_0(kr) j_0(kr') \left\{ \frac{1}{(e_Q + M)^2} + \frac{1}{(e_{\bar{q}} + m)^2} \right\},
\end{aligned} \tag{15}$$

where $e_Q = \sqrt{M^2 + k^2/4}$ and $e_{\bar{q}} = \sqrt{m^2 + k^2/4}$. This relation implies that the static approximation to the spin-orbit interaction in (6) represents a considerable overestimate of the net spin-orbit interaction in the case of light constituent quarks.

A similar more accurate representation of the quadratic spin-orbit component of the confining interaction obtains with the replacement

$$\begin{aligned}
\frac{1}{16M^2 m^2} \frac{c}{r^3} Q_{12} &\rightarrow -\frac{2c}{\pi r} \frac{\partial}{\partial r} \frac{1}{r} \frac{\partial}{\partial r} \int_0^\infty dr' r'^3 \\
& \int_0^\infty dk k^2 \frac{j_0(kr) j_0(kr')}{(e_Q + M)^2 (e_{\bar{q}} + m)^2}.
\end{aligned} \tag{16}$$

The \vec{p}^2 expansion of the interaction is an asymptotic series, which has to be truncated. As in the case of constituent quarks the successive terms have increasing amplitudes of alternating signs, this series is but a poor representation of the full spinorial structure of the interaction, the velocity dependence of which is well behaved. We shall therefore truncate the interaction to second order and retain only the local spin-orbit and quadratic spin-orbit interaction terms of quartic order. The latter is numerically insignificant for the low angular momentum states considered here.

To this order the most realistic treatment of the velocity dependent correction $-3/2\vec{p}^2/m_2^2$ to the linear potential cr in (6) would be to take it into account as a mass shift,

$$m^* \rightarrow m^* + \frac{3}{2}cr\left(\frac{m^*}{m_2}\right)^2, \quad (17)$$

in the kinetic term in (6). We shall treat this reduction of the kinetic term phenomenologically by subtraction of a constant (b) from the kinetic term. The value of this constant is determined by a fit of the calculated spectra to the experimental one. Without such a constant the kinetic term in the Hamiltonian becomes unrealistically large as becomes evident below.

3.2 The one-gluon exchange interaction

In the case of heavy quarkonia the perturbative gluon exchange interaction forms an important component of the hyperfine interaction between quarks [18]. To second order in the inverse quark masses (with exception for the quadratic spin-orbit interaction, which is quartic) that interaction, after multiplication of the square root factors in (3), takes the form:

$$\begin{aligned} V_G = & -\frac{4}{3}\alpha_s \left\{ \frac{1}{r} - \frac{3\pi}{2m_2^2}\delta^{(3)}(r) + \frac{\vec{p}^2}{2Mmr} \right\} \\ & + \frac{8\pi}{9} \frac{\alpha_s}{Mm} \delta^{(3)}(r) \vec{\sigma}_Q \cdot \vec{\sigma}_{\bar{q}} + \frac{\alpha_s}{3Mmr^3} S_{12} \\ & + \frac{2\alpha_s}{3r^3} \left\{ \frac{M^2 + m^2}{2M^2m^2} + \frac{2}{Mm} \right\} \vec{S} \cdot \vec{L} \\ & - \frac{\alpha_s}{6r^3} \frac{M^2 - m^2}{M^2m^2} (\vec{\sigma}_Q - \vec{\sigma}_{\bar{q}}) \cdot \vec{L} + \frac{\alpha_s}{4r^5 M^2 m^2} Q_{12}. \end{aligned} \quad (18)$$

Here the mass coefficient m_2 is defined in (7). Note that without the square root factors in (3) the numerical coefficients in the last two terms in the first bracket on the r.h.s. would be $-\pi$ and 1 instead of $-3\pi/2$ and $1/2$ respectively.

For light quarkonia the static gluon exchange interaction (18) has only qualitative value in view of the slow convergence of the asymptotic expansion in v/c . Moreover the quadratic spin-orbit interaction is ill-behaved in this limit. A more realistic version of this interaction is obtained by replacing the main $1/r$ (and the accompanying δ function term) by the corresponding unapproximated form:

$$-\frac{4}{3} \frac{\alpha_s}{r} \rightarrow -\frac{4}{3} \frac{f_0(r)}{r}. \quad (19)$$

Here the function $f_0(r)$ is defined as

$$f_0(r) = \frac{2}{\pi} \int_0^\infty dk \frac{\sin(kr)}{k} \frac{M}{e_Q} \frac{m}{e_{\bar{q}}} \left(\frac{M+m}{e_Q + e_{\bar{q}}} \right) \alpha_s(k^2). \quad (20)$$

The factors e_Q and $e_{\bar{q}}$ are defined as

$$e_Q = \sqrt{M^2 + \frac{k^2}{4}}, \quad e_{\bar{q}} = \sqrt{m^2 + \frac{k^2}{4}}. \quad (21)$$

Here $\alpha_s(k^2)$ is the running coupling constant of QCD, for which we use the screened parametrization [27]

$$\alpha_s(k^2) = \frac{12\pi}{27} \frac{1}{\ln[(k^2 + 4m_g^2)/\Lambda_0^2]}. \quad (22)$$

The corresponding modification of the \vec{p}^2/r term in (18) is obtained by the replacement

$$-\frac{4}{3}\alpha_s \frac{\vec{p}^2}{2Mmr} \rightarrow -\frac{4}{3} \frac{f_2(r)}{r} \vec{p}^2, \quad (23)$$

where

$$\begin{aligned} f_2(r) = & \frac{2}{\pi} \int_0^\infty dk \frac{\sin(kr)}{k} \left(\frac{e_Q + M}{2e_Q} \right) \left(\frac{e_{\bar{q}} + m}{2e_{\bar{q}}} \right) \left(\frac{M + m}{e_Q + e_{\bar{q}}} \right) \\ & \left\{ \frac{4}{(e_Q + M)(e_{\bar{q}} + m)} - \frac{1}{2e_Q e_{\bar{q}}} + \frac{1}{(e_Q + M)^2} \left[1 - \frac{M(e_Q + M)}{2e_Q^2} \right] \right. \\ & \left. + \frac{1}{(e_{\bar{q}} + m)^2} \left[1 - \frac{m(e_{\bar{q}} + m)}{2e_{\bar{q}}^2} \right] \right\} \alpha_s(k^2). \end{aligned} \quad (24)$$

It is necessary to treat this term exactly in the solution of the wave equation and not as a first order perturbation. The unapproximated version of the spin-spin component of the gluon exchange interaction is introduced by the replacement of the delta function as

$$\alpha_s \delta^{(3)}(r) \rightarrow \frac{1}{2\pi^2 r} \int_0^\infty dk k \sin(kr) \left(\frac{M + m}{e_Q + e_{\bar{q}}} \right) \frac{Mm}{e_Q e_{\bar{q}}} \alpha_s(k^2). \quad (25)$$

The unapproximated forms for the tensor and spin-orbit interactions in (18) are

$$V_G(T) = \frac{2}{9\pi} S_{12} \int_0^\infty dk k^2 j_2(kr) \left(\frac{M + m}{e_Q + e_{\bar{q}}} \right) \frac{\alpha_s(k^2)}{e_Q e_{\bar{q}}}. \quad (26)$$

$$\begin{aligned} V_G(LS) = & \frac{2}{3\pi r} \vec{S} \cdot \vec{L} \int_0^\infty dk k j_1(kr) \left(\frac{M + m}{e_Q + e_{\bar{q}}} \right) \frac{e_Q + M}{e_Q} \frac{e_{\bar{q}} + m}{e_{\bar{q}}} \\ & \left\{ \frac{1}{(e_{\bar{q}} + m)^2} \left[1 - \frac{k^2}{4(e_Q + M)^2} \right] + \frac{1}{(e_Q + M)^2} \left[1 - \frac{k^2}{4(e_{\bar{q}} + m)^2} \right] \right. \\ & \left. + \frac{4}{(e_Q + M)(e_{\bar{q}} + m)} \right\} \alpha_s(k^2). \end{aligned} \quad (27)$$

The integrals in the spin-spin and tensor interactions above are strongly moderated when the running coupling strength $\alpha_s(k^2)$ is taken into account. The quadratic spin-orbit interaction component in (18) may be similarly regulated by employment of the unapproximated form

$$\frac{\alpha_s}{4r^5 M^2 m^2} \rightarrow \frac{2}{3\pi r^2} \int_0^\infty dk k^2 j_2(kr) \frac{\alpha_s(k^2)}{e_Q e_{\bar{q}} (e_Q + M)(e_{\bar{q}} + m)} \left(\frac{M + m}{e_Q + e_{\bar{q}}} \right). \quad (28)$$

This form of the quadratic spin-orbit interaction has finite matrix elements.

The parametrization (22) takes the long distance screening of the quark-gluon coupling into account through the gluon mass parameter m_g . For this we use the value $m_g = 240$ MeV while for the confinement scale parameter Λ_0 we use the value 280 MeV. These values are chosen by a fit to the heavy-light meson spectra below. They are similar to those used in refs. [27, 28].

The employment of the screened running quark-gluon coupling strength along with the relativistic corrections to the gluon exchange interaction leads to significant dampening of the gluon exchange interaction at short range. This is shown in Fig. 1, where the unapproximated values for $f_0(r)$ as given by the expression (19) are plotted for the case of D and B mesons with $M = 1.58$ GeV and 4.825 GeV respectively, and $m = 450$ MeV. The result reveals that the approximation $f_0(r) = \alpha_s = \text{constant}$ is inadequate. The parametrization (22) gives the value ~ 0.4 for α_s at the charmonium scale, which is consistent with the values extracted by lattice methods in refs. [25, 26]. In the numerical results for the spectra of the heavy-light mesons below, it proved essential to use the unapproximated expressions for the functions $f_0(r)$ and $f_2(r)$, the reason being that the small mass of the light quarks render the static approximations misleading.

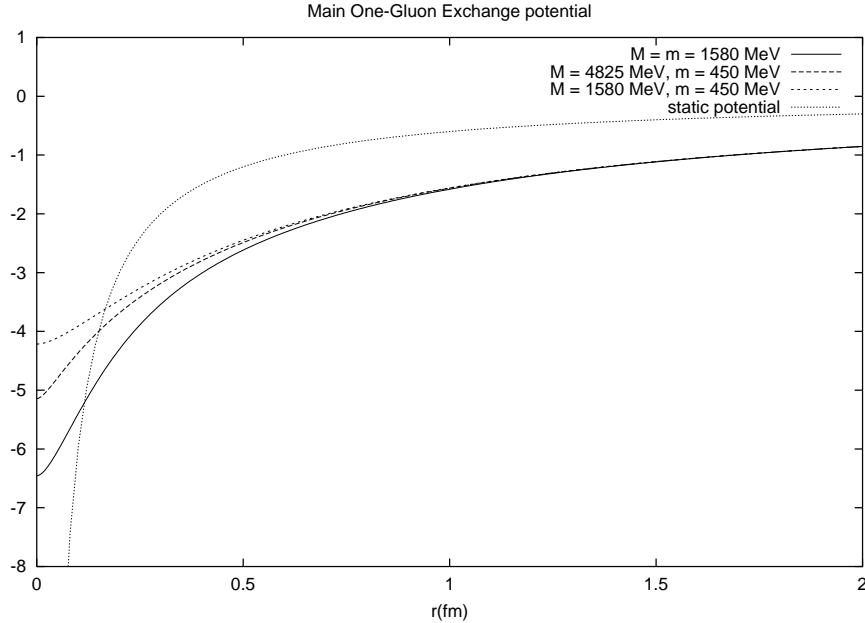


Figure 1: The exact function $-\frac{4}{3} \frac{f_0(r)}{r}$ calculated for several sets of heavy and light quark masses and compared to the static approximation for $\alpha_s = 0.45$

3.3 The instanton induced interaction

Numerical QCD lattice calculations indicate that the instanton liquid model provides an appropriate description of the dynamics in the low energy regime [2, 21, 22]. The instantons induce a pointlike interaction between heavy and light quarks, which contributes significantly to the hyperfine interaction in heavy-light

mesons [19].

The instanton induced interaction for $Q\bar{q}$ systems contains a color dependent component, which may be the cause of the splitting between light pseudoscalar and vector mesons, for which the color magnetic interaction is screened. The form of the instanton induced interaction, which is appropriate for heavy-light mesons has been derived in ref.[19], who considered the large N_c limit, where the matrix element of the color exchange operator is $\langle \lambda^1 \cdot \lambda^2 \rangle / 4 = -N_c/2$. The spin-dependent component of this interaction couples as a T invariant $\sigma_{\mu\nu}^1 \sigma_{\mu\nu}^2 / 2$, which implies that it may be viewed as a vector meson exchange like interaction with anomalous couplings to quarks.

If the large N_c limit is not invoked, the instanton induced interaction for the $Q\bar{q}$ system takes the form [19]:

$$H_{Q\bar{q}} = \left(\frac{\Delta M_Q \Delta m_q}{2nN_c} \right) \left(1 + \frac{1}{4} \lambda_Q \cdot \lambda_{\bar{q}} \right) \delta^{(3)}(r) - \frac{1}{4} \left(\frac{\Delta M_Q^{spin} \Delta m_{\bar{q}}}{2nN_c} \right) \vec{\sigma}_Q \cdot \vec{\sigma}_{\bar{q}} \lambda_Q \cdot \lambda_{\bar{q}} \delta^{(3)}(r) \quad (29)$$

Here n represents the instanton density, which typically is assigned the value 1 fm^{-4} . The mass parameters ΔM_Q , $\Delta m_{\bar{q}}$ and ΔM_Q^{spin} represent the mass shifts of the heavy (Q) and light (\bar{q}) quarks, which are caused by the instanton induced interaction. The numerical values for these mass shifts were obtained as $\Delta M_Q = 86 \text{ MeV}$, $\Delta M_Q^{spin} = 3 \text{ MeV}$ and $\Delta m_q = 420 \text{ MeV}$ respectively in ref. [19].

The expression (29) represents the approximate effective instanton induced interaction that obtains when one of the quarks is much heavier than the other one, which is appropriate here. The Lorentz structure of the main term in the interaction is a scalar, whereas the spin dependent term has a tensor coupling structure.

In the large color limit the sign of the spin-independent term in (29) is negative. In that limit the instanton induced interaction (29) plays a role akin to that of gluon exchange, with matrix elements of similar magnitude [19]. Without invocation of that limit, the spin-dependent term of the interaction (29) is not sufficiently strong to explain e.g. all of the difference between the D^* and D meson masses. As below it is found that the screened gluon exchange interaction described above provides sufficient splitting strength, the numerical results do not include the interaction (29). If the gluon mass parameter were increased, it would be necessary to include the additional spin-dependence given by the instanton induced interaction, however.

4 The spectra of charmonium and the heavy-light mesons

4.1 The charmonium spectrum

The mass of the charm quark was fixed by a fit to the D and D_S meson spectra, and then tested by direct computation of the $c\bar{c}$ spectrum, without further modification of the charm quark mass. The spectrum of charmonium is fairly well known experimentally.

The interaction model consists of the all the local terms in the scalar linear confining interaction (6),(8) and the gluon exchange interaction, with full account of the relativistic corrections and the running coupling strength as described in section (3.2) above.

The calculated spectrum is compared to the experimental spectrum in Table 2. The parameters in the interaction model are listed in Table 1. The value for the charm quark mass (1580 MeV) was chosen to be the same as that used for the D and D_S -mesons below. With the parameter values listed in Table 1 we are able to accurately reproduce the experimentally determined J/Ψ - η_c splitting, but at the price of 30-50 MeV overpredictions of the excited states. This effect is similar to that noted in [7]. Better agreement with experiment can be achieved by lowering the confining string constant to 960 MeV/fm and raising the gluon mass m_g by 20 MeV to 260 MeV. In this case the excited states agree fairly well with experiment, while the J/Ψ - η_c splitting is underpredicted by 15 MeV. A lower charm quark mass for the charmonium system would also improve the spectra, but as the charmonium spectrum is calculated primarily for testing purposes we keep the charm quark mass equal to that used for the D and D_S -mesons. We thus conclude that our test results for charmonium are similar to the spectrum obtained in [7].

	$c\bar{c}$	D_S	D
c	1120 MeV/fm	1120 MeV/fm	1120 MeV/fm
b	-50 MeV	-260 MeV	-320 MeV
Λ_0	280 MeV	280 MeV	280 MeV
m_g	240 MeV	240 MeV	240 MeV
m_c	1580 MeV	1580 MeV	1580 MeV
m_s	-	560 MeV	-
$m_{u,d}$	-	-	450 MeV

Table 1: Model parameters used for the charmonium, D and D_S meson spectra.

The quality of the spectrum is similar to that obtained with an effective interaction constructed by means of lattice methods [1], as well as by completely nonrelativistic phenomenology [29, 16]. The numerical values for the calculated energies of the $c\bar{c}$ are listed in Table 2, along with the experimental values [30].

	Predicted States (MeV)	Experimental states (MeV)
1^1S_0	2975	2979.8 ± 2.1
1^3S_1	3088	3096.88 ± 0.04
2^1S_0	3682	
2^3S_1	3736	3686.00 ± 0.09
1^1P_1	3518	
1^3P_0	3450	3417.3 ± 2.8
1^3P_1	3519	3510.53 ± 0.12
1^3P_2	3580	3556.17 ± 0.13

Table 2: Calculated and experimental charmonium states.

4.2 The D and D_s -meson spectra

In the calculation of the spectra of the D and D_s mesons, the constituent masses of the light and strange quarks are treated as phenomenological parameters to be fitted against the known splittings in the spectrum. While a reasonable overall description of the D meson spectrum is readily obtainable with the interaction models described above, a quantitative description of e.g. the spin-orbit splitting of the P-shell D_j ($j = 0, 1, 2$) D meson resonances demands a real effort.

The main difficulty with the spin orbit splittings may be ascribed to the small mass of the light quarks, which makes the matrix elements of the spin-orbit components of both the confining and hyperfine interactions large. That is the reason for taking into account the relativistic damping of these interaction components that is described in section 3.

	$M_{u,d}=450$ MeV	Exp(D^0)	Exp(D^\pm)
1^1S_0	1874	1864.6 \pm 0.5	1869.3 \pm 0.5
1^3S_1	2006	2006.7 \pm 0.5	2010.0 \pm 0.5
2^1S_0	2540		
2^3S_1	2601	2637 ?	2637 ?
3^1S_0	2904		
3^3S_1	2947		
4^1S_0	3175		
4^3S_1	3208		
1^1P_1	2389		
1^3P_0	2341		
1^3P_1	2407	2422.2 \pm 1.8	
1^3P_2	2477	2458.9 \pm 2.0	2459 \pm 4
2^1P_1	2792		
2^3P_0	2758		
2^3P_1	2802		
2^3P_2	2860		
3^1P_1	3082		
3^3P_0	3050		
3^3P_1	3085		
3^3P_2	3142		
1^1D_2	2689		
1^3D_1	2750		
1^3D_2	2727		
1^3D_3	2688		
2^1D_2	2997		
2^3D_1	3052		
2^3D_2	3029		
2^3D_3	2999		

Table 3: Calculated and experimental D -meson states.

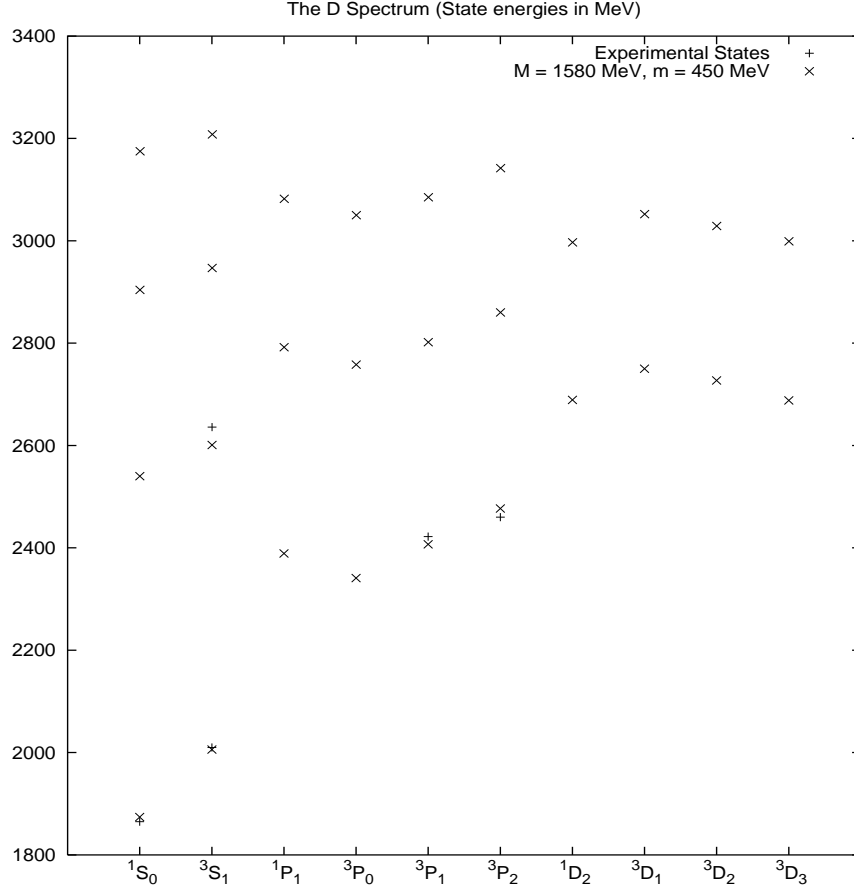


Figure 2: Calculated and experimental D -meson states.

The spectrum of the D meson that is obtained with the scalar linear confining interaction and with the quark masses $m_u = m_d = 450$ MeV and $m_c = 1580$ MeV is shown in Fig. 2. The light quark mass here is about 100 MeV larger than the typical values employed in nonrelativistic phenomenology. Reducing this mass further in the calculation would lead to an unrealistically large spin-orbit splitting of the P -states, while giving an unrealistically small $1S \rightarrow 2S$ spacing. The interaction parameters used in the calculation are listed in Table 1.

The calculated energies of the D -meson states are listed in Table 3 along with the known empirical energies [30].

The calculated D meson spectrum has the correct $D^* - D$ ground state splitting and only slightly underpredicts the possible D meson excitation [31] at 2637 MeV. The P -shell states around 2400 MeV are also well reproduced.

The calculated energies of the D_s meson states are shown in Fig. 3 and are listed in Table 4. As in the case of the D meson a satisfactory description of the still very incompletely known experimental spectrum is only achievable with a fairly large value for the constituent mass of the s quark ($m_s = 560$ MeV).

The overall structure of the D_s meson spectrum in Fig. 3 is similar to that of the D meson spectrum in Fig. 2. The ground state splitting is given correctly, as are the known P -state excitations.

The calculated D meson spectrum is similar to that obtained by the Gross

reduction of the Bethe-Salpeter equation in ref.[8]. The shell spacing at increasing energy of the latter is somewhat wider, which may reflect a difference between the different quasipotential reductions, but also the employment of static potentials in ref.[8].

	$M_s=560$ MeV	Experimental states (MeV)
1^1S_0	1975	1968.5 ± 0.6 2112.4 ± 0.7
1^3S_1	2108	
2^1S_0	2659	
2^3S_1	2722	
3^1S_0	3044	
3^3S_1	3087	
4^1S_0	3331	
4^3S_1	3364	
1^1P_1	2502	$2535.35 \pm 0.34 \pm 0.5$ 2573.5 ± 1.7
1^3P_0	2455	
1^3P_1	2522	
1^3P_2	2586	
2^1P_1	2928	
2^3P_0	2901	
2^3P_1	2942	
2^3P_2	2988	
3^1P_1	3234	
3^3P_0	3214	
3^3P_1	3244	
3^3P_2	3283	
1^1D_2	2838	
1^3D_1	2845	
1^3D_2	2856	
1^3D_3	2857	
2^1D_2	3144	
2^3D_1	3172	
2^3D_2	3167	
2^3D_3	3157	

Table 4: Calculated and experimental D_s -meson states.

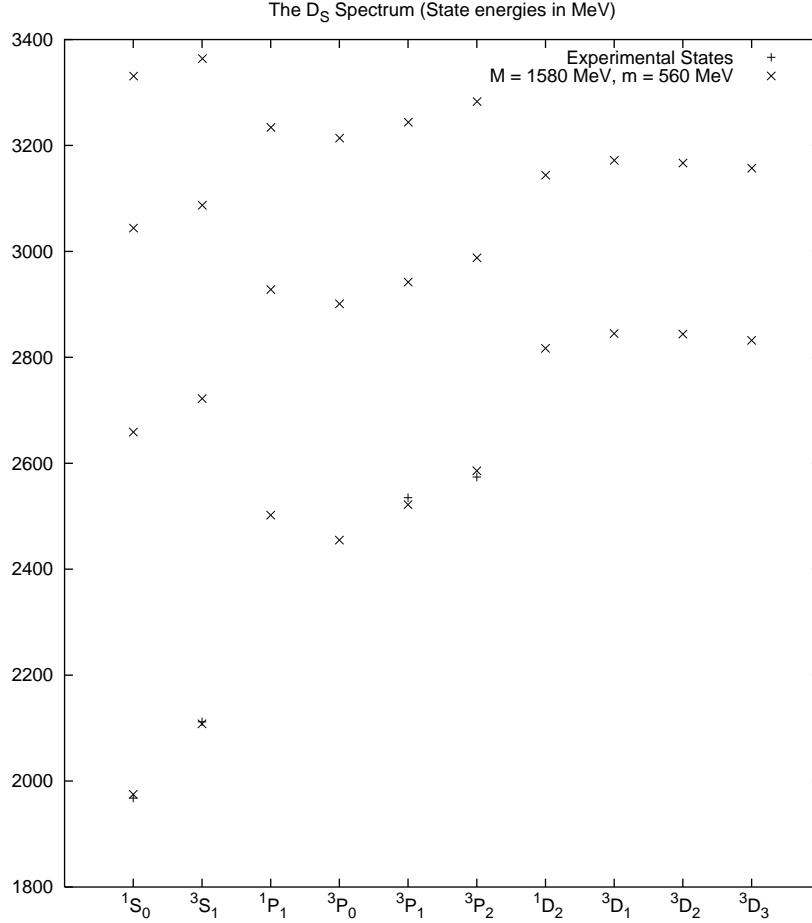


Figure 3: Calculated and experimental D_s meson states.

4.3 The B and B_s -meson spectra

The empirical knowledge of the spectra of the B and B_s mesons is still very incomplete. Only the ground state pseudoscalar and vector meson state energies are known with certainty. In addition one orbital excitation of the B meson is known at 5700 MeV, which presumably belongs to the P -shell.

The only additional parameter required to calculate the spectra of the bottom mesons with the interaction models described above is the b quark mass. For this we choose the value $m_b=4825$ MeV, with which value the pseudoscalar-vector splitting of the bottom and strange bottom mesons is obtained correctly.

The calculated B and B_s meson spectra are shown in Figs. 4 and 5. The energies of these states are also listed in Tables 6 and 7, along with the empirical values that are taken from ref.[30]. The orbital excitation of the B meson at 5700 MeV is obtained correctly, under the assumption that it corresponds to a $j = 1$ P -shell state.

The overall features of the calculated bottom meson spectra are similar to those obtained with the Gross reduction [7] of the Bethe-Salpeter equation in ref.[8], although as in the case of the charm mesons, we obtain somewhat smaller

shell spacings at higher excitation.

	B_s	B
c	1120 MeV/fm	1120 MeV/fm
b	-185 MeV	-250 MeV
Λ_0	280 MeV	280 MeV
m_g	240 MeV	240 MeV
m_b	4825 MeV	4825 MeV
m_s	560 MeV	-
$m_{u,d}$	-	450 MeV

Table 5: Parameter values used in the calculation of the B_S and B -meson spectra.

State	$M_{u,d}=450$ MeV	Exp(B^0)	Exp(B^\pm)
1^1S_0	5277	5279.2 \pm 1.8	5278.9 \pm 1.8
1^3S_1	5325	5324.9 \pm 1.8	
2^1S_0	5822		
2^3S_1	5848		
3^1S_0	6117		
3^3S_1	6136		
4^1S_0	6335		
4^3S_1	6351		
1^1P_1	5686		
1^3P_0	5678		
1^3P_1	5699	5697 \pm 9	
1^3P_2	5704		
2^1P_1	6022		
2^3P_0	6010		
2^3P_1	6028		
2^3P_2	6040		
3^1P_1	6259		
3^3P_0	6242		
3^3P_1	6260		
3^3P_2	6277		
1^1D_2	5920		
1^3D_1	6005		
1^3D_2	5955		
1^3D_3	5871		
2^1D_2	6179		
2^3D_1	6248		
2^3D_2	6207		
2^3D_3	6140		

Table 6: Calculated and experimental B -meson states

	$M_s=560$ MeV	Experimental B_S states (MeV)
1^1S_0	5366	5369.3 ± 2.0 5416.3 ± 3.3
1^3S_1	5417	
2^1S_0	5939	
2^3S_1	5966	
3^1S_0	6254	
3^3S_1	6274	
4^1S_0	6487	
4^3S_1	6504	
1^1P_1	5795	
1^3P_0	5781	
1^3P_1	5805	
1^3P_2	5815	
2^1P_1	6153	
2^3P_0	6143	
2^3P_1	6160	
2^3P_2	6170	
3^1P_1	6406	
3^3P_0	6396	
3^3P_1	6411	
3^3P_2	6421	
1^1D_2	6043	
1^3D_1	6094	
1^3D_2	6067	
1^3D_3	6016	
2^1D_2	6320	
2^3D_1	6362	
2^3D_2	6339	
2^3D_3	6298	

Table 7: Calculated and experimental B_s -meson states.

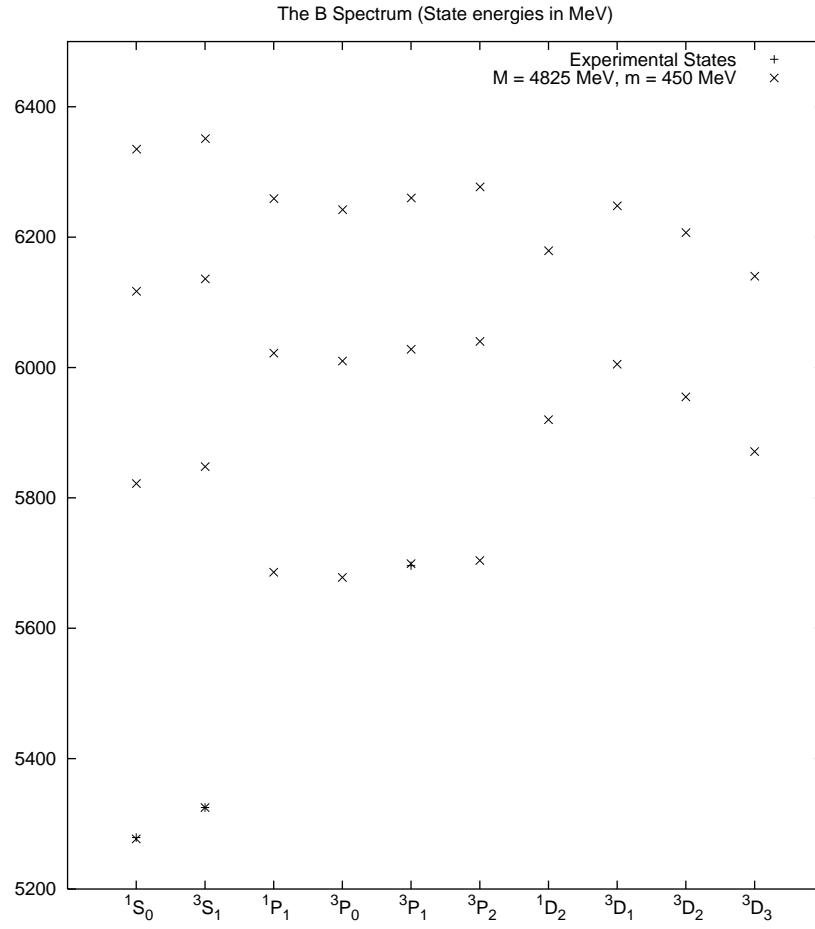


Figure 4: Calculated and experimental B -meson spectra.

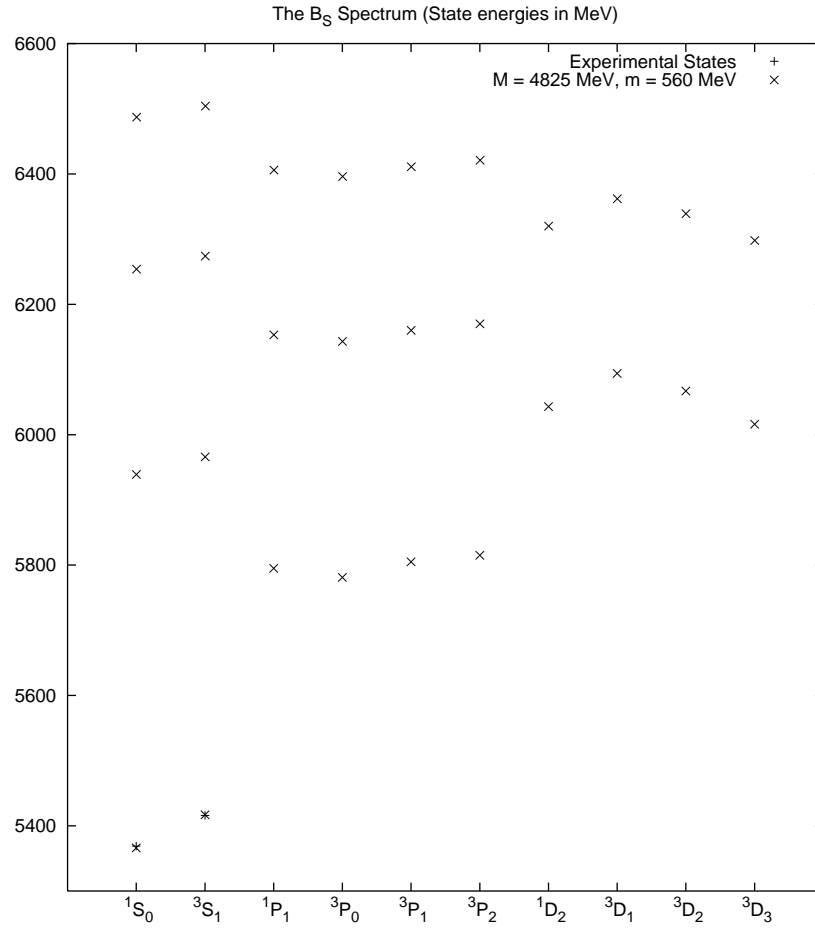


Figure 5: Calculated and experimental B_s -meson spectra.

5 Quark current operators

5.1 Single quark currents

In order to calculate the M1 transitions of the $Q\bar{q}$ systems we employ the full Dirac structure of the single quark current operators. This was shown to be necessary in ref.[16] for a satisfactory description of the corresponding M1 decays of heavy quarkonia. The current density operators of the constituent light quarks and the c and b quarks are then

$$\langle p' | \vec{j}(0) | p \rangle = iQ[\bar{u}(\vec{p}')\vec{\gamma}u(\vec{p})]. \quad (30)$$

Here Q is the quark charge operator, which takes the values $\pm 2e/3$ and $\pm e/3$. With canonical boosts for the quark spinors u, \bar{u} , this current operator leads to the magnetic moment operator

$$\vec{\mu} = Q \left(\frac{m_p}{m_Q} \right) \frac{\vec{\sigma}}{\sqrt{1+\vec{v}^2}} \left\{ 1 - \frac{1}{3} \left(1 - \frac{1}{\sqrt{1+\vec{v}^2}} \right) \right\} \mu_N, \quad (31)$$

where \vec{v} is the quark velocity: $\vec{v} = (\vec{p}' + \vec{p})/2m_Q$, m_p is the proton mass and μ_N is the nuclear magneton.

For the D^\pm mesons the spin flip part of the combination of the magnetic moments of the charm quark and the light antiquarks is

$$\begin{aligned} \vec{\mu}_{flip}(D^\pm) = & \pm \frac{1}{6} m_p (\vec{\sigma}_c - \vec{\sigma}_{\bar{d}}) \left\{ \frac{2}{m_c} \frac{1}{\sqrt{1+\vec{v}_c^2}} \left[1 - \frac{1}{3} \left(1 - \frac{1}{\sqrt{1+\vec{v}_c^2}} \right) \right] \right. \\ & \left. - \frac{1}{m_{\bar{d}}} \frac{1}{\sqrt{1+\vec{v}_{\bar{d}}^2}} \left[1 - \frac{1}{3} \left(1 - \frac{1}{\sqrt{1+\vec{v}_{\bar{d}}^2}} \right) \right] \right\} \mu_N. \end{aligned} \quad (32)$$

For the D^0, \bar{D}^0 mesons the corresponding operator is

$$\begin{aligned} \vec{\mu}_{flip}(D^0, \bar{D}^0) = & \pm \frac{1}{3} m_p (\sigma_c - \sigma_{\bar{u}}) \left\{ \frac{1}{m_c} \frac{1}{\sqrt{1+\vec{v}_c^2}} \left[1 - \frac{1}{3} \left(1 - \frac{1}{\sqrt{1+\vec{v}_c^2}} \right) \right] \right. \\ & \left. + \frac{1}{m_{\bar{u}}} \frac{1}{\sqrt{1+\vec{v}_{\bar{u}}^2}} \left[1 - \frac{1}{3} \left(1 - \frac{1}{\sqrt{1+\vec{v}_{\bar{u}}^2}} \right) \right] \right\} \mu_N. \end{aligned} \quad (33)$$

Here m is the mass of the light antiquark, and \vec{v}_c and $\vec{v}_{\bar{q}}$ denote the velocity operators of the charm quark and the light antiquark respectively. The spin-flip magnetic moment operator for the D_s^\pm meson may be obtained from the corresponding expression for the D^\pm mesons by replacing $\vec{\sigma}_{\bar{d}}, m_{\bar{d}}$ and $\vec{v}_{\bar{d}}$ in (32) by $\vec{\sigma}_{\bar{s}}, m_{\bar{s}}$ and $\vec{v}_{\bar{s}}$ respectively.

The spin-flip magnetic moment operators for the bottom mesons may be constructed by similar replacements. For the B^\pm mesons these operators are obtained from those for the D^\pm (32) by replacement of the c quark mass and velocity by the corresponding u quark mass and velocities and by replacement of the d quark mass and velocity by the b quark mass and velocity.

The spin-flip magnetic moment operator for the B^0 and \bar{B}^0 mesons is obtained from that for the neutral D mesons (33) by multiplying the operator by

$-1/2$ and by replacing the c and \bar{u} quark masses and velocities by the corresponding masses and velocities for the d and \bar{b} quark. A further replacement of the d quark mass and velocity by the corresponding s quark mass and velocity yields the spin-flip magnetic moment operator for the B_s mesons.

Note that when matrix elements of these magnetic moment operators are evaluated with wave functions that are solutions to the Blankenbecler-Sugar equation (1), these operators should be multiplied by the factor

$$f_{BS} = \frac{M + m}{M\sqrt{1 + v_Q^2} + m\sqrt{1 + v_{\bar{q}}^2}}. \quad (34)$$

5.2 Two-quark currents

Both the scalar confining interaction and the hyperfine interaction may excite virtual quark-antiquark states, which are deexcited by the electromagnetic field. This process is illustrated by the Feynman diagrams in Fig.6. These operators may be derived by the methods described in ref.[16].

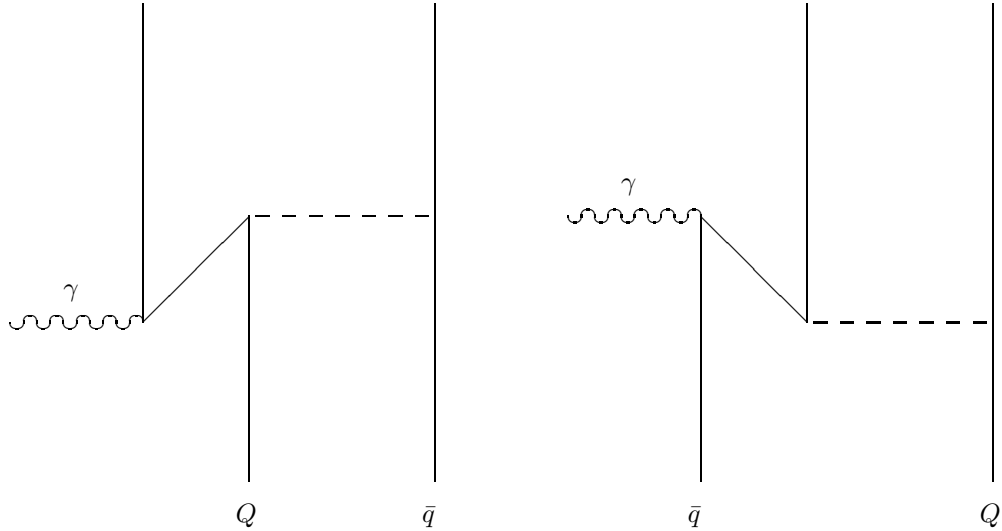


Figure 6: Exchange current operators associated with the effective scalar confining and gluon exchange interactions, with intermediate virtual $q\bar{q}$ excitations.

For the D^\pm system the two-quark current that is implied by the scalar confining interaction to lowest order in v/c takes the form

$$\vec{j}_2(C) = \mp i e c r \frac{m_p}{12} \left(\frac{2}{m_c^2} - \frac{1}{m_d^2} \right) (\vec{\sigma}_c - \vec{\sigma}_d) \times \vec{q}. \quad (35)$$

This current operator may be viewed as a direct renormalization of the corresponding spin-flip combination of the single c and \bar{d} current operators:

$$\vec{j}_{c\bar{d}} = \pm i e \frac{m_p}{12} \left(\frac{2}{m_c^2} - \frac{1}{m_d^2} \right) (\vec{\sigma}_c - \vec{\sigma}_d) \times \vec{q}. \quad (36)$$

The two-quark magnetic moment operator that is implied by this current operator is then accordingly

$$\vec{\mu}_2(C) = \mp cr \frac{m_p}{6} \left\{ \frac{2}{m_c^2} - \frac{1}{m_{\bar{d}}^2} \right\} (\sigma_c - \sigma_{\bar{d}}) \mu_N. \quad (37)$$

For the D^0, \bar{D}^0 mesons the corresponding two-quark magnetic moment is then

$$\vec{\mu}_2(C) = \mp cr \frac{m_p}{3} \left\{ \frac{1}{m_c^2} - \frac{1}{m_{\bar{u}}^2} \right\} (\sigma_c - \sigma_{\bar{u}}) \mu_N. \quad (38)$$

The exchange magnetic moment operator for the D_s^\pm mesons is obtained from that for the D^\pm mesons (37), by replacing $\vec{\sigma}_{\bar{d}}$ and $m_{\bar{d}}$ by $\vec{\sigma}_{\bar{s}}$ and $m_{\bar{s}}$ respectively.

The general rule is that the exchange current that is associated with the confining interaction has opposite sign to the corresponding combination of single quark current operators, and may be obtained directly from the former by multiplication by the factor $-cr$ and by squaring the quark masses in the denominators. The corresponding operators for the bottom mesons are readily constructed with the help of this rule. Note that the constant b , which is subtracted from the Hamiltonian, is viewed as an approximation to the velocity dependent term $-3/2 \vec{p}^2/m_2^2$ in the confining interaction (6). As that term may be viewed as the origin for the two-quark interaction current that is associated with the scalar confining interaction through the continuity equation, it should not be subtracted from the cr term in the two-body current.

The gluon exchange interaction (18) also implies a two-quark exchange current operator. The matrix elements of this two-body current are however significantly weaker than those of the exchange current operator that is associated with the scalar confining operator [16]. Because of the cancellations between the matrix elements of the single quark current operators and those of the exchange current operator that is associated with the confining interaction, the gluon exchange current operator does give a significant contribution to the calculated M1 transition rates between the ground state heavy-light mesons.

For the D^\pm mesons this two-quark current, to lowest order in the inverse quark masses, has the form

$$\begin{aligned} \vec{j}_2(G) [D^\pm] = & \pm e \frac{8\pi}{9} \left\{ \frac{2\alpha_s(k_{\bar{d}}^2)}{3k_{\bar{d}}^2} \left[\frac{\vec{p}_{\bar{d}} + \vec{p}_{\bar{d}}'}{m_c m_{\bar{d}}} \right. \right. \\ & + i \left(\frac{\vec{\sigma}_c}{m_c^2} + \frac{\vec{\sigma}_{\bar{d}}}{m_c m_{\bar{d}}} \right) \times \vec{k}_{\bar{d}} \\ & \left. \left. + \frac{\alpha_s(k_c^2)}{3k_c^2} \left[\frac{\vec{p}_c + \vec{p}_c'}{m_c m_{\bar{d}}} + i \left(\frac{\vec{\sigma}_c}{m_c m_{\bar{d}}} + \frac{\vec{\sigma}_{\bar{d}}}{m_c^2} \right) \times \vec{k}_c \right] \right\}. \quad (39) \end{aligned}$$

Here the momentum operators $\vec{k}_{\bar{d}}$ and \vec{k}_c denote the fractional momenta imparted to the \bar{d} and c (or d and \bar{c}) quarks respectively.

The spin-flip component of the magnetic moment operator, that is obtained from this current operator, is then

$$\begin{aligned} \vec{\mu}_2(G) [D^\pm] = & \pm \frac{f_0(r)}{27} \frac{m_p}{r} \left(\frac{2}{m_c^2} - \frac{1}{m_c m_{\bar{d}}} - \frac{1}{m_{\bar{d}}^2} \right) \\ & (\vec{\sigma}_c - \vec{\sigma}_{\bar{d}}) \mu_N. \quad (40) \end{aligned}$$

In the case of the D^0 and \bar{D}^0 mesons the gluon exchange current operator takes the form

$$\begin{aligned} \vec{j}_2(G) [D^0, \bar{D}^0] = & \pm e \frac{16\pi}{27} \left\{ \frac{\alpha_s(k_u^2)}{k_u^2} \left[\frac{\vec{p}_u' + \vec{p}_{\bar{u}}}{m_c m_{\bar{u}}} \right. \right. \\ & + i \left(\frac{\vec{\sigma}_c}{m_c^2} + \frac{\vec{\sigma}_{\bar{u}}}{m_c m_{\bar{u}}} \right) \times \vec{k}_{\bar{u}} \\ & \left. \left. - \frac{\alpha_s(k_c^2)}{k_c^2} \left[\frac{\vec{p}_c' + \vec{p}_c}{m_c m_{\bar{u}}} + i \left(\frac{\vec{\sigma}_c}{m_c m_{\bar{u}}} + \frac{\vec{\sigma}_{\bar{u}}}{m_{\bar{u}}^2} \right) \times \vec{k}_c \right] \right\}. \end{aligned} \quad (41)$$

The corresponding spin-flip magnetic moment operator is

$$\vec{\mu}_2(G) [D^0, \bar{D}^0] = \pm \frac{2f_0(r)}{27} \frac{m_p}{r} \left(\frac{1}{m_c^2} - \frac{1}{m_{\bar{u}}^2} \right) (\vec{\sigma}_c - \vec{\sigma}_{\bar{u}}) \mu_N. \quad (42)$$

The gluon exchange spin-flip magnetic moment for the D_s^\pm mesons is obtained from that for the D^\pm mesons (40) by replacing $\vec{\sigma}_{\bar{d}}$ and $m_{\bar{d}}$ by $\vec{\sigma}_{\bar{s}}$ and $m_{\bar{s}}$ respectively.

The gluon exchange spin-flip magnetic moment operator for the B^- and B^+ mesons is obtained from the corresponding expressions (42) for the D^0 and \bar{D}^0 mesons by replacing the c quark mass and spin operator by the b quark mass and spin operator. Similarly by replacing the c quark mass and spin operator in the expressions (40) for the D^+ and D^- gluon exchange spin-flip magnetic moment operator by the b quark mass and spin operator one obtains the corresponding operator for the \bar{B}^0 and B^0 mesons. Finally the expressions for the gluon exchange spin-flip magnetic moment for the \bar{B}_s^0 and B_s^0 mesons are obtained from those for the D_s^+ and D_s^- mesons by the replacement of the c quark mass and spin operator by the b quark mass and spin operator.

The exchange magnetic moments that are associated with the confining and gluon exchange interactions above represent relativistic corrections of second order in v/c , as is implied by their origin as pair excitation currents (Fig. 6). They thus appear in the same order as the relativistic corrections to the single quark magnetic moment operators. As relativistic corrections to the exchange current operators are of quartic order in v/c we have not considered them here, in order to be consistent with the treatment of the confining interaction without quartic terms in v/c , besides the numerically insignificant quadratic spin-orbit interaction.

6 M1 transitions

6.1 M1 transition matrix elements for D mesons

The spin-flip component of all the magnetic moment operators derived above may be written in the general form

$$\vec{\mu} = e\mathcal{M}(\vec{\sigma}_Q - \vec{\sigma}_{\bar{q}}). \quad (43)$$

Here \mathcal{M} is the matrix element of the orbital part of the magnetic moment operator between the initial and final meson states. The transition width for M1 transitions of the type $Q\bar{q}(J=1) \rightarrow Q\bar{q}(J=0)\gamma$ may be expressed as

$$\Gamma = \frac{16}{3} \alpha_{em} \frac{M_f}{M_i} \mathcal{M}^2 q^3. \quad (44)$$

Here α_{em} is the fine structure constant and q is the photon momentum in the laboratory frame. The masses of the initial and final meson states are denoted M_i and M_f respectively.

The matrix element \mathcal{M} is defined as the coefficient of the spin-flip operator $\vec{\sigma}_c - \sigma_{\bar{q}}$ in the expression for the magnetic moment operator. It is formed as a sum of matrix elements of single quark and exchange magnetic moment operators. In the case of the D^\pm mesons, the matrix element between S -states of the single quark operator (32) may be written in the form

$$\begin{aligned} \mathcal{M}_{IA}(D^\pm) = & \pm \frac{1}{3} \int_0^\infty dp p^2 \int_{-1}^1 dz f_{BS}(p) \int_0^\infty dr' r'^2 \int_0^\infty dr r^2 \varphi_f(r') \\ & \left\{ \frac{2}{m_c \sqrt{1+v_c^2}} \left[1 - \frac{1}{3} \left(1 - \frac{1}{\sqrt{1+v_c^2}} \right) \right] \right. \\ & \left. - \frac{1}{m_{\bar{d}} \sqrt{1+v_{\bar{d}}^2}} \left[1 - \frac{1}{3} \left(1 - \frac{1}{\sqrt{1+v_{\bar{d}}^2}} \right) \right] \right\} \\ & j_0 \left(r' \sqrt{p^2 + pqz/2 + q^2/16} \right) j_0 \left(r \sqrt{p^2 - pqz/2 + q^2/16} \right) \varphi_i(r) \end{aligned} \quad (45)$$

Here $v_c = p/m_c$, $v_{\bar{d}} = p/m_{\bar{d}}$, and the factor $f_{BS}(p)$ is the “minimal relativity” factor (34). The expression for corresponding matrix elements in the case of the D^0 and \bar{D}^0 systems is readily inferred from eqn (33) by comparison. Here $\varphi_i(r)$ and $\varphi_f(r')$ denote the initial and final orbital wavefunctions respectively.

It is instructive to compare these expressions to those of the static quark model ($v_c, v_{\bar{d}} \rightarrow 0$). In the case of the D^\pm mesons that expression is simply

$$\mathcal{M}_{IA}(D^\pm) = \pm \frac{1}{12} \int_0^\infty d^3r \varphi_f^*(r) \left(\frac{2}{m_c} - \frac{1}{m_{\bar{d}}} \right) j_0 \left(\frac{qr}{2} \right) \varphi_i(r) \quad (46)$$

whereas for the D^0, \bar{D}^0 systems it is

$$\mathcal{M}_{IA}(D^0, \bar{D}^0) = \pm \frac{1}{6} \int_0^\infty d^3r \varphi_f^*(r) \left(\frac{1}{m_c} + \frac{1}{m_{\bar{u}}} \right) j_0 \left(\frac{qr}{2} \right) \varphi_i(r). \quad (47)$$

The expressions (45) and (46) apply to D_s^\pm mesons with the substitutions $m_{\bar{d}} \rightarrow m_{\bar{s}}$ and $v_{\bar{d}} \rightarrow v_{\bar{s}}$.

The matrix elements of the exchange magnetic moment that is associated with the confining interaction (6) is in the case of the D^\pm mesons

$$\mathcal{M}_2(C) = \mp \frac{1}{12} c \int_0^\infty d^3r r \varphi_f^*(r) \left(\frac{2}{m_c^2} - \frac{1}{m_{\bar{d}}^2} \right) j_0 \left(\frac{qr}{2} \right) \varphi_i(r). \quad (48)$$

This expression applies to the D_s^\pm mesons as well, with the substitution $m_{\bar{d}} \rightarrow m_{\bar{s}}$. In the case of the D_0, \bar{D}_0 mesons the corresponding expression is

$$\mathcal{M}_2(C) = \mp \frac{1}{6} c \int_0^\infty d^3r r \varphi_f^*(r) \left(\frac{1}{m_c^2} + \frac{1}{m_{\bar{u}}^2} \right) j_0 \left(\frac{qr}{2} \right) \varphi_i(r). \quad (49)$$

The matrix element of the gluon exchange spin-flip magnetic moment operator is in the case of the D^\pm mesons (cf.(40)):

$$\mathcal{M}_2(G) = \pm \frac{1}{54} \left(\frac{2}{m_c^2} - \frac{1}{m_c m_{\bar{d}}} - \frac{1}{m_{\bar{d}}^2} \right) \int_0^\infty d^3 r \varphi_f^*(r) \frac{f_0(r)}{r} j_0 \left(\frac{qr}{2} \right) \varphi_i(r). \quad (50)$$

In the case of the D^0, \bar{D}^0 mesons this matrix element is

$$\mathcal{M}_2(G) = \pm \frac{1}{27} \left(\frac{1}{m_c^2} + \frac{1}{m_{\bar{u}}^2} \right) \int_0^\infty d^3 r \varphi_f^*(r) \frac{f_0(r)}{r} j_0 \left(\frac{qr}{2} \right) \varphi_i(r). \quad (51)$$

The rule for constructing the corresponding matrix element expressions for the other heavy-light meson charge states may be inferred from these expressions.

6.2 M1 transitions of charm mesons

At present the only experimental information on the M1 transition rates of D -meson states are the M1 branching ratios for $D^*(2010)^\pm \rightarrow D^\pm \gamma$: $1.1^{+2.1}_{-0.7}\%$ and for $D^*(2007)^0 \rightarrow D^0 \gamma$: $38.1 \pm 2.9\%$ [30]. As the upper limit for the total width of the former transition is 0.131 MeV and for the latter 2.1 MeV, the upper limits for the M1 decay widths are accordingly 1.44 keV for $D^*(2010)^\pm \rightarrow D^\pm \gamma$ and 800 keV for $D^*(2007)^0 \rightarrow D^0 \gamma$. These upper limits suggest that the M1 decay widths should be of the order 1 keV.

	NRIA	RIA	RIA + cf.	RIA + cf. + ex.
$D^{*0} \rightarrow D^0$	20.9 keV	6.52 keV	2.21 keV	1.25 keV
$D^{*'} \rightarrow D^0$	805 eV	51.1 keV	39.3 keV	44.5 keV
$D^{*'} \rightarrow D'^0$	1.88 keV	631 eV	2.48 keV	2.24 keV
$D'^0 \rightarrow D^{*0}$	3.02 keV	35.7 keV	31.6 keV	34.2 keV

Table 8: The M1 decay widths of the D_0 ($c\bar{u}$) mesons

	NRIA	RIA	RIA + cf.	RIA + cf. + ex.
$D^{*\pm} \rightarrow D^\pm$	574 eV	10.8 eV	2.09 keV	1.10 keV
$D^{*'} \rightarrow D^\pm$	23.9 eV	2.77 keV	12.5 keV	15.7 keV
$D^{*'} \rightarrow D'^\pm$	52.6 eV	2.84 eV	748 eV	607 eV
$D'^\pm \rightarrow D^{*\pm}$	85.3 eV	1.63 keV	10.2 keV	11.9 keV

Table 9: The M1 decay widths of the D^\pm ($c\bar{d}$) mesons

This is indeed what we find by explicit calculation here. The calculated widths for the transitions $D^*(2010)^\pm \rightarrow D^\pm \gamma$ and $D^*(2007)^0 \rightarrow D^0 \gamma$, as well as for the transitions between their respective excited states are listed in Tables 9 and 8 respectively. The first column gives the nonrelativistic impulse approximation results (NRIA), which are obtained with static quark current operators. The experience from the corresponding decays in charmonium suggests that these are not realistic. The results obtained in the relativistic impulse approximation, with the full Dirac magnetic moment operators are listed in the second column (RIA). These values should also, on the basis of the experience

	NRIA	RIA	RIA + cf.	RIA + cf. + ex.
$D_s^* \rightarrow D_s$	178 eV	7.10 meV	736 eV	337 eV
$D_s^{*'} \rightarrow D_s$	7.88 eV	1.22 keV	3.26 keV	4.47 keV
$D_s^{*'} \rightarrow D_s'$	17.1 eV	246 meV	258 eV	200 eV
$D_s' \rightarrow D_s^*$	22.4 eV	654 eV	2.53 keV	3.13 keV

Table 10: The M1 decay widths of the D_s ($c\bar{s}$) mesons

with heavy quarkonia, be unrealistic. Finally the column RIA + c.f. give the results that are obtained when the exchange current contribution that is associated with the scalar confining interaction is taken into account. The last column (RIA + c.f. + ex.) also takes into account the contribution of the gluon exchange current. The contribution of the latter is most significant for the M1 transitions between the ground states.

In Tables 9 and 8 the M1 transition between the excited D^* and D mesons and the ground states are given as well. In the case of the forbidden transitions between the orbitally excited states the two-body current contributions are dominant. The large difference between the calculated M1 transition rates of the charged and neutral D -mesons is due to the very different quark mass dependence of the associated spin-flip magnetic moment operators. In the derivation of these results we determined the value of the photon momentum q from the differences between the empirical values for the D meson states as given in ref.[30]. The difference is only notable in the case of the excited D' and D'^* mesons, the latter of which is underpredicted by about 35 MeV.

We have also calculated the M1 transition rates for $J/\psi \rightarrow \eta_c \gamma$ and $\psi' \rightarrow \eta_c \gamma$ with the present framework and parameters. In this case the gluon exchange current does not contribute at all because of the equal masses of the charm quarks and antiquarks. The empirical width for the $J/\psi \rightarrow \eta_c \gamma$ decay is known to be 1.14 ± 0.39 keV. For this we find the value 0.75 keV when the two-body contribution is included, while the relativistic impulse approximation value is 1.47 keV. The static quark model prediction is 2.51 keV, which amounts to an overprediction of about a factor 2. The empirical width of the forbidden M1 transition $\psi' \rightarrow \eta_c \gamma$ is 0.78 ± 0.24 keV. For this we obtain the value 1.49 keV when the two-body current is taken into account. This is much closer to the empirical value than the value 0.17 keV given by the static quark model or the value 8.48 keV that is obtained in the relativistic impulse approximation.

The M1 calculated transitions between the D_s^* and D_s mesons are listed in Table 10. These transition rates should *a priori* be expected to be qualitatively similar to those of the $D^{*\pm}$ and D^\pm mesons. This is borne out by the calculation, although the numerical values show marked differences. This is another illustration of the sensitivity of the calculated M1 transition rates to the parameters of the model and in this case to the difference between the constituent masses of the s and d quarks.

6.3 M1 transitions of bottom mesons

The calculated M1 transition widths of the bottom mesons are listed in Tables 11 and 12. The experimental decay widths for these transitions are yet to be measured. The large masses of the bottom mesons make these transition widths much smaller than those of the corresponding transitions of charm mesons.

The overall features of these results are however similar to those of the

charm mesons. The nonrelativistic impulse approximation leads to considerable overestimates. In the case of the forbidden transitions the two-body exchange currents are again dominant.

The calculated M1 transition rates for the strange bottom mesons are listed in Table 13.

	NRIA	RIA	RIA + cf.	RIA + cf. + ex.
$B^{*0} \rightarrow B^0$	152 eV	51.9 eV	25.1 eV	9.55 eV
$B^{*'}0 \rightarrow B^0$	149 meV	5.39 keV	9.73 keV	12.2 keV
$B^{*'}0 \rightarrow B'^0$	27.7 eV	9.59 eV	48.3 eV	40.6 eV
$B^{0'} \rightarrow B^{*0}$	34.6 eV	4.31 keV	7.95 keV	9.72 keV

Table 11: The M1 decay widths of the B_0 ($b\bar{d}$) mesons

	NRIA	RIA	RIA + cf.	RIA + cf. + ex.
$B^{*\pm} \rightarrow B^\pm$	462 eV	132 eV	160 eV	67.4 eV
$B^{*'\pm} \rightarrow B^\pm$	455 meV	20.1 keV	39.2 keV	50.9 keV
$B^{*'\pm} \rightarrow B'^\pm$	84.3 eV	24.6 eV	221 eV	183 eV
$B'^\pm \rightarrow B^{*\pm}$	105 eV	15.8 keV	32.4 keV	40.7 keV

Table 12: The M1 decay widths of the B^\pm ($b\bar{u}$) mesons

	NRIA	RIA	RIA + cf.	RIA + cf. + ex.
$B_s^* \rightarrow B_s$	116 eV	46.4 eV	945 meV	148 meV
$B_s^{*'} \rightarrow B_s$	2.39 eV	3.87 keV	2.29 keV	3.22 keV
$B_s^{*'} \rightarrow B_s'$	20.9 eV	8.26 eV	12.4 eV	9.76 eV
$B_s' \rightarrow B_s^*$	10.6 eV	3.12 keV	1.84 keV	2.50 keV

Table 13: The M1 decay widths of the B_s ($b\bar{s}$) mesons

7 Discussion

The main result of the present study is that it is possible to achieve a satisfactory description of the heavy-light meson spectra, as well as credible predictions for their radiative spin-flip transitions with the framework of the Blankenbecler-Sugar equation with a scalar confining interaction. This conclusion differs from that in ref.[11]. The calculated results are however very sensitive to the parameters in the model, and to the relativistic damping of the hyperfine interaction. This suggests that that model for the hyperfine interaction (relativistic gluon exchange) may not provide a sufficiently complete description of the hyperfine interaction. It may be conjectured that screening the gluon exchange interaction at shorter distances and compensating with the instanton induced interaction may lead to less parameter sensitive results.

Both the Blankenbecler-Sugar and Gross quasipotential reductions of the Bethe-Salpeter equation lead to two-body exchange current operators, which connect to negative energy intermediate states. If the confining interaction couples as a scalar to the quarks, the accompanying two-quark magnetic moment is a pure spin-flip operator for mesons with equal quark and antiquark masses. The contribution of this operator is essential for obtaining realistic M1 transition rates for heavy quarkonia [16]. In the equal mass case the analog two-quark operator that arises with a vector confining interaction has no spin-flip component [32].

For mesons with unequal quark and antiquark masses the gluon exchange current operator has a spin-flip component. It therefore also contributes to the M1 decay rates of the heavy-light mesons. Although this contribution is much smaller than that of the confining interaction, it is significant in the case of the M1 transitions between the ground state vector and pseudoscalar heavy-light mesons, because of the partial cancellation between the matrix elements of the single quark current operators and those of the exchange current associated with the confining interaction.

Strong conclusions concerning the M1 transition rates here have to await experimental determination of the total width of the heavy-flavor vector mesons. As the relative branching ratios for M1 decays of these mesons are known, the key missing empirical information is their total widths for strong decay.

Acknowledgments

This work has been supported in part by Academy of Finland under contract 43982.

References

- [1] G. S. Bali, K. Schilling and A. Wachter, Phys. Rev. **56**, 2566 (1997)
- [2] D. Diakonov and V. Petrov, eprint hep-lat/9810037
- [3] B. Metsch, Nucl. Phys. **A578**, 418 (1994)
- [4] J. Linde and H. Snellman, Nucl. Phys. **A619**, 346 (1997)
- [5] R. Blankenbecler and R. Sugar, Phys. Rev. **142**, 1051 (1966)
- [6] A.A. Logunov and A.N. Tavkhelidze, Nuovo Cimento **29**, 380 (1963)
- [7] F. Gross, Phys. Rev. **186**, 1448 (1969)
- [8] J. Zeng, J. W. Van Orden and W. Roberts, Phys. Rev. **D52**, 5229 (1995)
- [9] F. Coester and D. O. Riska, Ann. Phys. **234**, 141 (1994)
- [10] M. H. Partovi and E. H. Lomon, Phys. Rev. **D2**, 1999 (1980)
- [11] D. Ebert, V. O. Galkin and R. Faustov, Phys. Rev. **D57**, 5663 (1998), **D59**, 1019902 (1999)
- [12] G. E. Brown, A. D. Jackson and T. T. S. Kuo, Nucl. Phys. **A133**, 481 (1969)

- [13] J. F. Amundson et al., Phys. Lett. **B296**, 415 (1992)
- [14] L. Angelos and G. P. Lepage, Phys. Rev. **D45**, R3021 (1992)
- [15] B. Bajc, S. Fajfer and R. J. Oakes, Phys. Rev. **D51**, 2230 (1995)
- [16] T.A. Lähde, C. Nyfält and D.O. Riska, Nucl. Phys. **A645**, 587 (1999)
- [17] D. Gromes, Phys. Lett. **B202**, 262 (1988)
- [18] S. Godfrey and N. Isgur, Phys. Rev. **D32**, 189 (1985)
- [19] S. Chernyshev, M.A. Nowak and I. Zahed, Phys. Rev. **D53**, 5176 (1996)
- [20] M. A. Nowak, M. Rho and I. Zahed, *Chiral Nuclear Dynamics*, World Scientific, Singapore (1996)
- [21] M.-C. Chu et al., Phys. Rev. **D49**, 6039 (1994)
- [22] J. W. Negele, Nucl. Phys. Proc. Suppl. **73**, 92 (1999)
- [23] D. Ebert, R. N. Faustov and V. O. Galkin, Eur. Phys. Journal **C7**, 539 (1999)
- [24] D. O. Riska, Nucl. Phys. **B56**, 445 (1973)
- [25] C. T. H. Davies et al., Phys. Lett. **B345**, 42 (1996)
- [26] C. T. H. Davies et al., Phys. Rev. **D56**, 2755 (1997)
- [27] A. C. Mattingly and P. M. Stevenson, Phys. Rev. **D49**, 437 (1994)
- [28] S. J. Brodsky, C.-R. Ji, A. Pang and D. G. Robertson, Phys. Rev. **D57**, 245 (1998)
- [29] E. J. Eichten and C. Quigg, Phys. Rev. **D52**, 1726 (1995)
- [30] C. Caso et al., Eur. Phys. Journal **C3**, 1 (1998)
- [31] C. Bourdarios, eprint hep-ex/9811014
- [32] K. Tsushima, D. O. Riska and P. G. Blunden, Nucl. Phys. **A559**, 543 (1993)